

Are your MRI contrast agents cost-effective?

Learn more about generic Gadolinium-Based Contrast Agents.



AJNR

¹⁸F-Fluorodeoxyglucose Positron Emission Tomography and MR Imaging Findings in Rasmussen Encephalitis

David J. Fiorella, James M. Provenzale, R. Edward Coleman, Barbara J. Crain and AbdulAziz Al-Sugair

This information is current as of April 19, 2024.

AJNR Am J Neuroradiol 2001, 22 (7) 1291-1299
<http://www.ajnr.org/content/22/7/1291>

¹⁸F-Fluorodeoxyglucose Positron Emission Tomography and MR Imaging Findings in Rasmussen Encephalitis

David J. Fiorella, James M. Provenzale, R. Edward Coleman, Barbara J. Crain, and AbdulAziz Al-Sugair

BACKGROUND AND PURPOSE: Rasmussen encephalitis is a chronic, progressive encephalitis that manifests as an abrupt-onset, intractable seizure disorder in previously developmentally normal children. The objectives of the current study were to characterize the ¹⁸F-fluorodeoxyglucose (FDG) positron emission tomography (PET) and MR imaging findings in Rasmussen encephalitis and to test the hypotheses that data from both imaging techniques are required to establish the diagnosis and identify the affected cerebral hemisphere in some cases.

METHODS: Eleven patients with Rasmussen encephalitis were identified from a review of a computer database. The MR (n = 10) and PET (n = 11) imaging data were reviewed retrospectively and conjointly.

RESULTS: On MR images, nine of 10 patients manifested bilateral cerebral atrophy that predominantly involved one hemisphere. One patient had purely unilateral cerebral atrophy. We observed foci of abnormally increased T2 signal intensity in nine of 10 patients. On FDG PET images, all patients showed extensive regions of hypometabolism within the cerebral hemisphere that showed the greatest atrophy. Discrete foci of hypermetabolism, indicative of seizure activity, were observed in six patients. The FDG PET and MR imaging findings were either stable or gradually progressive in patients with multiple imaging studies (MR, n = 5; FDG PET, n = 5).

CONCLUSION: Rasmussen encephalitis is characterized by diffuse, unilateral cerebral hypometabolism on FDG PET images, with corresponding regions of cerebral atrophy on MR images. Although MR imaging data alone are sufficient to suggest a diagnosis of Rasmussen encephalitis in many cases, correlation with FDG PET data increases diagnostic confidence and allows the unequivocal identification of the affected cerebral hemisphere in patients whose MR imaging findings are subtle or distributed bilaterally.

Rasmussen encephalitis is a chronic, progressive encephalitis of unknown etiology that results in severe, intractable epilepsy. Seizures typically are the focal motor type and begin abruptly in previously normal children. Characteristically, motor function deteriorates, often resulting in hemiparesis or hemiplegia as well as progressive cognitive decline (1–5).

Despite the widespread application of MR imaging and ¹⁸F-fluorodeoxyglucose (FDG) positron

emission tomography (PET) to evaluate patients with epilepsy, the findings on MR or FDG PET images in Rasmussen encephalitis have not been characterized definitively. Because of the absence of an established pattern of neuroimaging findings in Rasmussen encephalitis, confirmation based upon diagnosis relies heavily on a typical clinical presentation with histopathologic results from brain biopsy. Unfortunately, pathologic data sometimes are nondiagnostic or inconsistent. This may be attributed to sampling error and to evolution of the disease to a “burned-out” phase, which is characterized by nonspecific histopathologic features (3). Thus, in some patients, as the disease evolves, brain biopsy may become increasingly nondiagnostic. For this reason, neuroimaging data can play a critical role in establishing a diagnosis of Rasmussen encephalitis and in selecting patients for, and directing, brain biopsy.

The objectives of the current study were to characterize the FDG PET and MR imaging findings in Rasmussen encephalitis and to test the hypothesis that FDG PET data are required, in some cases, to

Received January 25, 2000; accepted after revision March 19, 2001.

From the Department of Radiology (D.J.F., J.M.P., R.E.C., A.A.-S.), Duke University Medical Center, Durham, NC, and the Department of Pathology (B.J.C.), The Johns Hopkins University School of Medicine, Baltimore, MD.

This work was presented in part at the 2000 American Roentgen Ray Society annual meeting, Washington, D.C., May 7–12.

Address reprint requests to David Fiorella, Duke University Medical Center, Box 3808 Medical Center, Durham, NC 27710.

© American Society of Neuroradiology

Surgical interventions and corresponding histopathologic results

Patient	Procedure	Lymphocytic		Microglial	Diagnosis
		Cuffing	Gliosis	Nodules	
1	Right frontal lobe resection	+	-	-	Perivascular chronic inflammation
2	Biopsy left temporal lobe	-	-	-	No inflammation
	Right hemispherectomy	+	+	+	Rasmussen encephalitis
3	Biopsy right superior temporal lobe	-	-	-	No inflammation
	Biopsy right inferior frontal lobe	+	-	-	Non-specific encephalitis
	Right hemispherectomy	+	+	+	Rasmussen encephalitis
4	Left hemispherectomy	+	+	+	Rasmussen encephalitis
5	Biopsy left frontal lobe	-	+	-	Gliosis, mild nonspecific encephalitis
	Left hemispherectomy	-	-	-	No pathologic diagnosis
6	Biopsy left temporal lobe	+	-	+	Rasmussen encephalitis
	Right hemispherectomy	+	-	-	Scant mononuclear perivascular inflammation
7	Biopsy left frontal + temporal lobe	+	+	+	Rasmussen encephalitis
	Biopsy left frontal lobe	+	+	-	Scant perivascular lymphocytic infiltrate, mild subpial gliosis
8	Biopsy	+	+	+	Rasmussen encephalitis
	Left hemispherectomy	+	+	+	Rasmussen encephalitis
9	Biopsy	+	+	-	Rasmussen encephalitis
10	Right hemispherectomy	+	-	+	Rasmussen encephalitis
11	Biopsy	+	+	-	Rasmussen encephalitis

establish the diagnosis and unequivocally identify the involved cerebral hemisphere.

Methods

Patients

We identified patients referred for evaluation of "seizure disorder" and those specifically referred for suspected clinical diagnosis of Rasmussen encephalitis by review of a computerized FDG PET database (1989 to 1998). Inclusion criteria were 1) clinical presentation consistent with Rasmussen encephalitis, as indicated by a diagnosis of "Rasmussen encephalitis" or "suspected Rasmussen encephalitis" recorded in clinical notes or discharge summaries; and 2) brain biopsy or brain resection specimen consistent with either "Rasmussen encephalitis" (n = 9) or the sequela of a "burned-out encephalitis" lacking another specific pathologic diagnosis (n = 2). Patients with "burned-out" encephalitis were included only when clinical features overwhelmingly suggested the diagnosis of Rasmussen encephalitis.

MR Imaging

The MR images were obtained with a 1.5-T scanner. Imaging sequences included spin-echo T1- (500–600/8–12 [TR/TE]) and T2- (TR, 2200–3000; TE, 30–40/80–100) weighted images in the axial plane; T2-weighted fast spin-echo with flow compensation, fast spoiled gradient-recalled, and fluid-attenuated inversion recovery imaging in the coronal oblique planes; and, in some cases, postcontrast T1-weighted images (500–600/8–12 [TR/TE]) in the coronal and axial planes (0.1 ml/kg gadopentate dimeglumine given intravenously [Magnevist; Berlex Laboratories, Wayne, NJ]). Field of view ranged from 22 to 24 cm, slice thickness was 5 mm, interslice gap was 2.5 mm, there were two excitations, and the matrix was 256 × 192. All MR imaging data were retrospectively and conjointly reviewed by two observers (D.J.F., J.M.P.) who were not blinded to the diagnosis.

¹⁸F-Fluorodeoxyglucose Positron Emission Tomography

All patients had nothing by mouth for 4 hours before intravenous administration of FDG (140 μCi/kg). The FDG was given in a quiet, dimly lit room; patients had their eyes open

and ears unoccluded. The patients remained in this environment for 30 minutes after FDG administration and then were positioned for the PET scan. Continuous EEG monitoring was performed during the radiopharmaceutical injection and uptake phase in seven of the 11 patients. Patients were imaged with a GE 4096 Plus or a GE Advance tomograph (GE Medical Systems, Milwaukee, WI). We acquired transaxial data and corrected the emission data using calculated attenuation correction. The data were displayed as transaxial, coronal, and sagittal images. All FDG PET imaging data were retrospectively and conjointly reviewed by three observers (D.J.F., A.A.-S., R.E.C.) who were not blinded to the diagnosis. There was no significant variance from the original interpretations.

Results

Patients

The age of seizure onset for the series of patients (five male, six female) ranged from 15 months to 8 years (average, 4.9 years). The age at initial MR imaging ranged from 32 months to 22 years (average, 8.5 years). The average interval between the first MR imaging examination and the corresponding FDG PET examination was 29.4 days (range, 0–131 days). Seven of 11 patients underwent hemispherectomy, and the remaining four patients underwent biopsy, limited resection, or both (Table). All patients undergoing hemispherectomy had a marked reduction in seizure activity (average follow-up, 41.4 months; range, 22–70 months). After hemispherectomy, three patients became seizure-free and required no antiepileptic medications, three patients became seizure-free but were maintained on one antiepileptic medication (patients 4, 5, and 10), and one patient (patient 2) initially became seizure-free, but more than 2 years after the surgery began to have occasional seizures.

In all patients, surgical intervention was performed on the cerebral hemisphere exhibiting hypometabolism on FDG PET images. We assigned

a pathologic diagnosis of Rasmussen encephalitis in nine patients on the basis of histologic findings. Tissue specimens from the remaining two patients (patients 1 and 5) showed features of mild, non-specific inflammation (patient 1) or gliosis (patient 5) but lacked features required for a specific pathologic diagnosis of encephalitis.

In two patients, initial brain biopsy was negative for evidence of significant encephalitis, but the histopathologic results from subsequent hemispherectomy were positive for all three characteristic findings of Rasmussen encephalitis: microglial nodules, gliosis, and perivascular lymphocytic cuffing. In addition, initial brain biopsy obtained from two patients showed characteristic findings of Rasmussen encephalitis, but the later histopathologic analysis showed only mild perivascular lymphocytic cuffing and gliosis, respectively. These patients (patients 6 and 7) underwent hemispherectomy following a substantial interval after the initial, unequivocally positive brain biopsy results (4 and 5 years, respectively) compared with the other patients. During this interval, one of these patients (patient 7) received intravenous immunoglobulin therapy.

Magnetic Resonance Imaging

Atrophy.—MR imaging data were available for 10 patients. Nine patients had bilateral cerebral atrophy. In one patient (patient 10), cerebral atrophy was solely unilateral. Seven patients showed bilateral but asymmetrical atrophy on the initial imaging study. Two patients developed bilateral atrophy after their initial study had showed either no atrophy (patient 2) or unilateral atrophy (patient 6).

In all patients, the observed atrophy was asymmetrical and predominantly involved the cerebral hemisphere that was hypometabolic on FDG PET images (Figs 1–4). The right hemisphere was predominantly affected in four patients and the left hemisphere in six patients. In seven patients, atrophy was distributed diffusely within the affected hemisphere. In three of the 10 patients (patients 6, 7, and 8), marked regions of focal atrophy were superimposed on the diffuse cerebral hemispheric atrophy (Fig 2). In two patients, T2-weighted images showed these regions of focal atrophy to have abnormally increased signal intensity within the cortical gray matter and subcortical white matter (Fig 2). Atrophy progressed in three of the five patients who underwent multiple studies (Fig 3).

Signal Abnormality on T2-weighted Sequences.—Nine patients showed abnormal foci of the T2 signal within the more atrophic cerebral hemisphere. These foci were distributed within the cortical gray matter of eight patients (Figs 2 and 3). Nine patients had hyperintense T2 signal distributed within the white matter of the affected cerebral hemisphere. In three patients (patients 3, 6, and 11), abnormal T2 signal was distributed within the white matter bilaterally (Fig 3). We noted signal

abnormality within the deep gray matter structures in two patients. None of the patients undergoing imaging after contrast medium administration showed abnormal contrast enhancement.

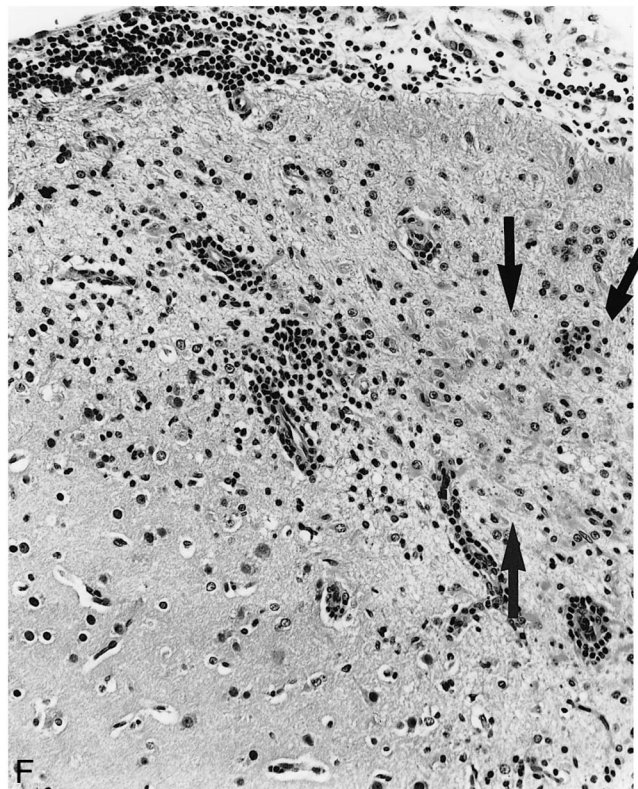
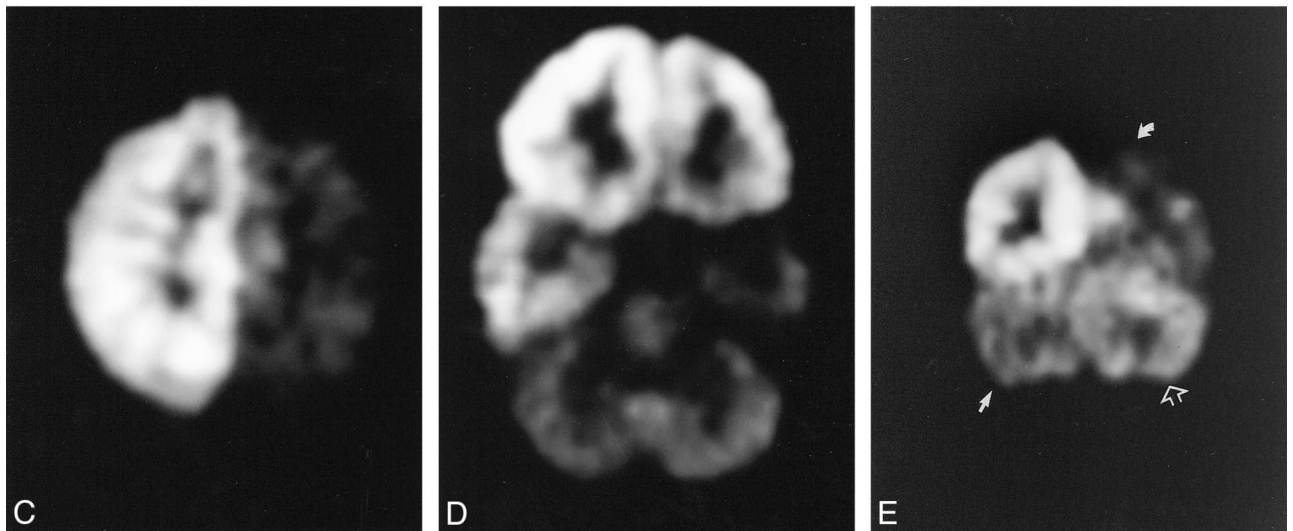
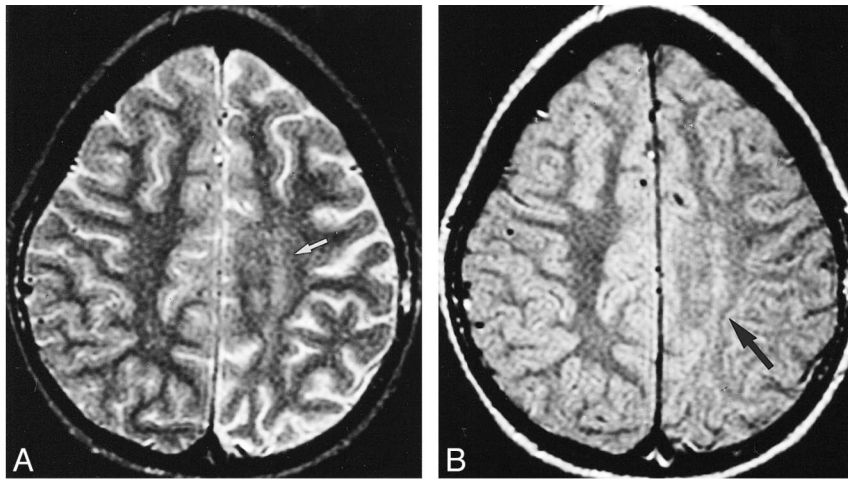
Hippocampal Formation.—The MR examinations were sufficient to evaluate the hippocampus in eight patients. Three patients had abnormally increased T2 signal intensity, and six showed atrophy, within the hippocampal formation of the predominantly involved hemisphere (Fig 3). Three patients had both atrophy and T2 signal hyperintensity within the affected hippocampus. Two patients had normal hippocampal anatomy and signal intensity.

¹⁸F-Fluorodeoxyglucose Positron Emission Tomography

FDG PET showed diffuse hypometabolism within one cerebral hemisphere in all 11 patients, distributed within the frontal (n = 10), parietal (n = 11), temporal (n = 11), and occipital (n = 6) lobes, respectively (Figs 1–5). Multiple examinations were available for five patients; in three, the regions of hypometabolism were stable, but the other two patients showed mild progression during the interval. The left hemispheric hypometabolism observed in patient 11 became less prominent on examination 1 year later. We noted foci of hypermetabolism, indicative of ictal foci, in six patients (Figs 3 and 5). Multiple examinations were available for three of these patients, and in each, the foci of hypermetabolism either completely (two patients) or partially (one patient) resolved on follow-up examinations. Three patients with foci of cerebral hypermetabolism also showed foci of hypermetabolism in the contralateral cerebellar hemisphere (Figs 3 and 5). During interictal studies, six patients showed hypometabolism in the contralateral cerebellar hemisphere, ie, crossed cerebellar diaschisis (Fig 1E). The ipsilateral basal ganglia showed regions of hypometabolism in four patients during interictal imaging and hypermetabolism in one patient during ictal imaging (Fig 3).

Discussion

In 1958, Rasmussen et al (1) presented a series of 27 patients who had a syndrome characterized by the abrupt onset of intractable focal seizures; these were children with previously normal development (1–5). The seizure disorder typically was accompanied by progressive motor and cognitive deterioration. Brain biopsy specimens obtained from these patients showed focal or unilateral “chronic encephalitis”, which included perivascular cuffs of lymphocytes around large and small vessels, microglial nodules within both gray and white matter, and gliosis (2, 3). The etiology of Rasmussen encephalitis remains unknown. An initial hypothesis proposed infection with a slow viral



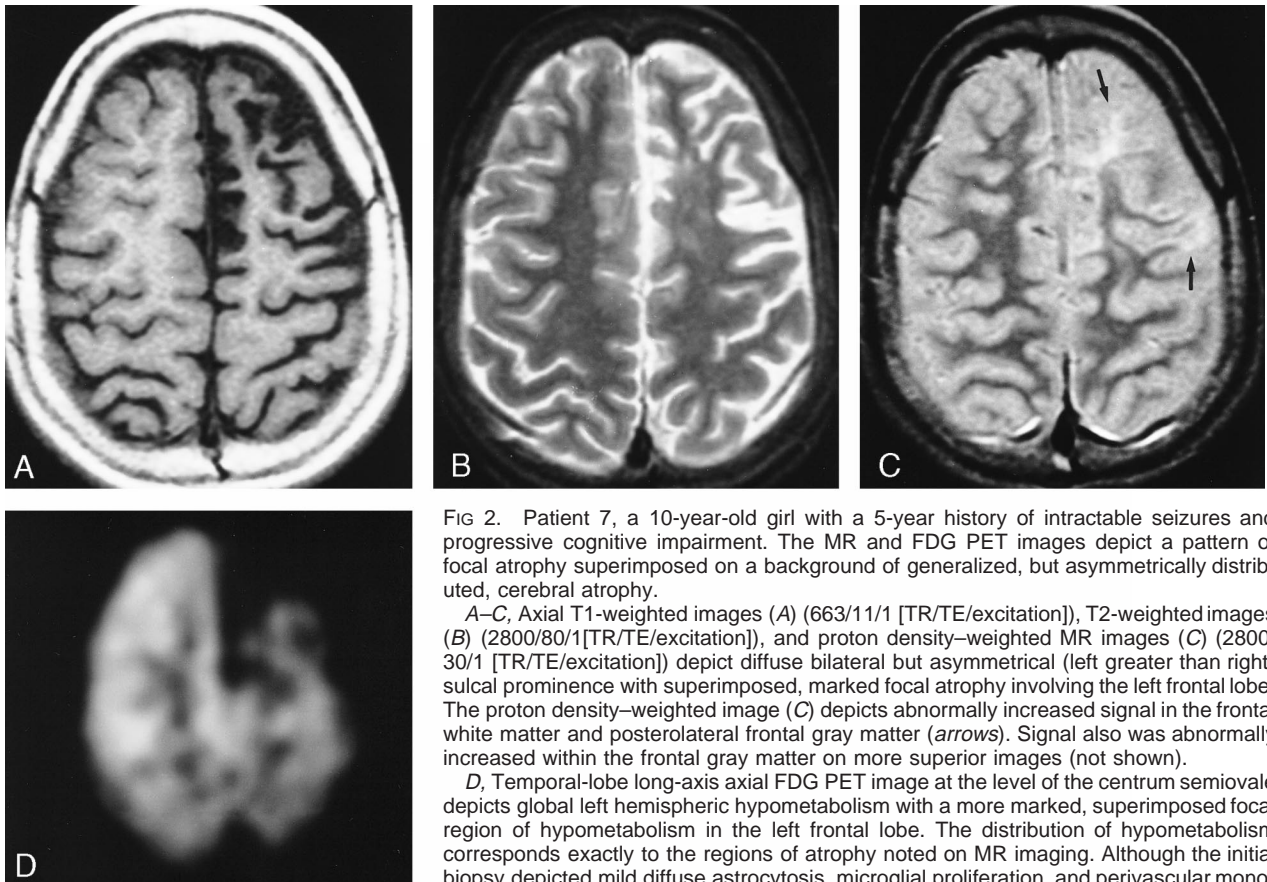


FIG 2. Patient 7, a 10-year-old girl with a 5-year history of intractable seizures and progressive cognitive impairment. The MR and FDG PET images depict a pattern of focal atrophy superimposed on a background of generalized, but asymmetrically distributed, cerebral atrophy.

A–C, Axial T1-weighted images (A) (663/11/1 [TR/TE/excitation]), T2-weighted images (B) (2800/80/1 [TR/TE/excitation]), and proton density-weighted MR images (C) (2800/30/1 [TR/TE/excitation]) depict diffuse bilateral but asymmetrical (left greater than right) sulcal prominence with superimposed, marked focal atrophy involving the left frontal lobe. The proton density-weighted image (C) depicts abnormally increased signal in the frontal white matter and posterolateral frontal gray matter (*arrows*). Signal also was abnormally increased within the frontal gray matter on more superior images (not shown).

D, Temporal-lobe long-axis axial FDG PET image at the level of the centrum semiovale depicts global left hemispheric hypometabolism with a more marked, superimposed focal region of hypometabolism in the left frontal lobe. The distribution of hypometabolism corresponds exactly to the regions of atrophy noted on MR imaging. Although the initial biopsy depicted mild diffuse astrocytosis, microglial proliferation, and perivascular mononuclear infiltration, a biopsy 4 years later depicted findings of “nonspecific encephalitis”. This may reflect either “sampling error” or progression to a “burned-out” phase of Rasmussen encephalitis.

agent (2). More recent studies have suggested an autoimmune mechanism (6).

Medical treatment has not controlled the seizures or significantly affected disease progression in these patients. As a result, many patients are treated surgically with functional hemispherectomy, ie, resection of the affected cerebral hemisphere (while sparing the frontal or occipital lobes) following division of connections to the brain stem and commissures, in an attempt to achieve seizure control (7).

Establishing a diagnosis of Rasmussen encephalitis is challenging. Clinically, Rasmussen encephalitis is a diagnosis of exclusion in patients with intractable seizures and progressive motor and cognitive deterioration, which may be verified by brain biopsy. However, as indicated by previous reports (3) as well as our results, biopsy results frequently are nondiagnostic, and repeated biopsies may yield conflicting results (Table). Two potential confounding factors may account for this fact. First, the site of biopsy within the affected cerebral hemisphere

←

FIG 1. Patient 2, a 7-year-old girl with a 2-year history of 20 to 30 focal partial motor and sensory seizures a day.

A, Axial T2-weighted image (2200/80/0.75 [TR/TE/excitation]) depicts bilateral cerebral atrophy distributed asymmetrically (left greater than right). Abnormally increased T2 signal is distributed within the white matter of the left centrum semiovale (*arrow*).

B, Axial proton density-weighted MR image (2200/30/0.75 [TR/TE/excitation]) depicts abnormally increased signal intensity within the posterior white matter bilaterally, left greater than right (*arrow*).

C and D, Axial ¹⁸F-Fluorodeoxyglucose (FDG) Positron Emission Tomography (PET) images at the level of the centrum semiovale (C) and suprasellar cistern (D) show marked hypometabolism throughout the left cerebral hemisphere, with some sparing of the inferior left frontal lobe.

E, Coronal FDG PET image depicts diffuse left cerebral (*curved arrow*) and right cerebellar (*closed arrow*) hypometabolism, ie, crossed cerebellar diaschisis. The left cerebellar hemisphere shows normal glucose metabolism (*open arrow*). Because of the compelling clinical presentation and neuroimaging findings, this patient underwent left hemispherectomy despite a nondiagnostic brain biopsy. Histopathologic findings obtained from the hemispherectomy specimen were consistent with Rasmussen encephalitis (Table).

F, The hemispherectomy specimen shows marked chronic inflammation, including lymphocytic meningitis (*top*), perivascular cuffing by lymphocytes, and an intraparenchymal lymphocytic infiltrate (hematoxylin and eosin stain, ×368). Neuronal loss and reactive astrocytosis are most apparent on the right side of the field (*arrows*). The discordance between the biopsy and hemispherectomy specimens likely reflects “sampling error” in the initial biopsy.

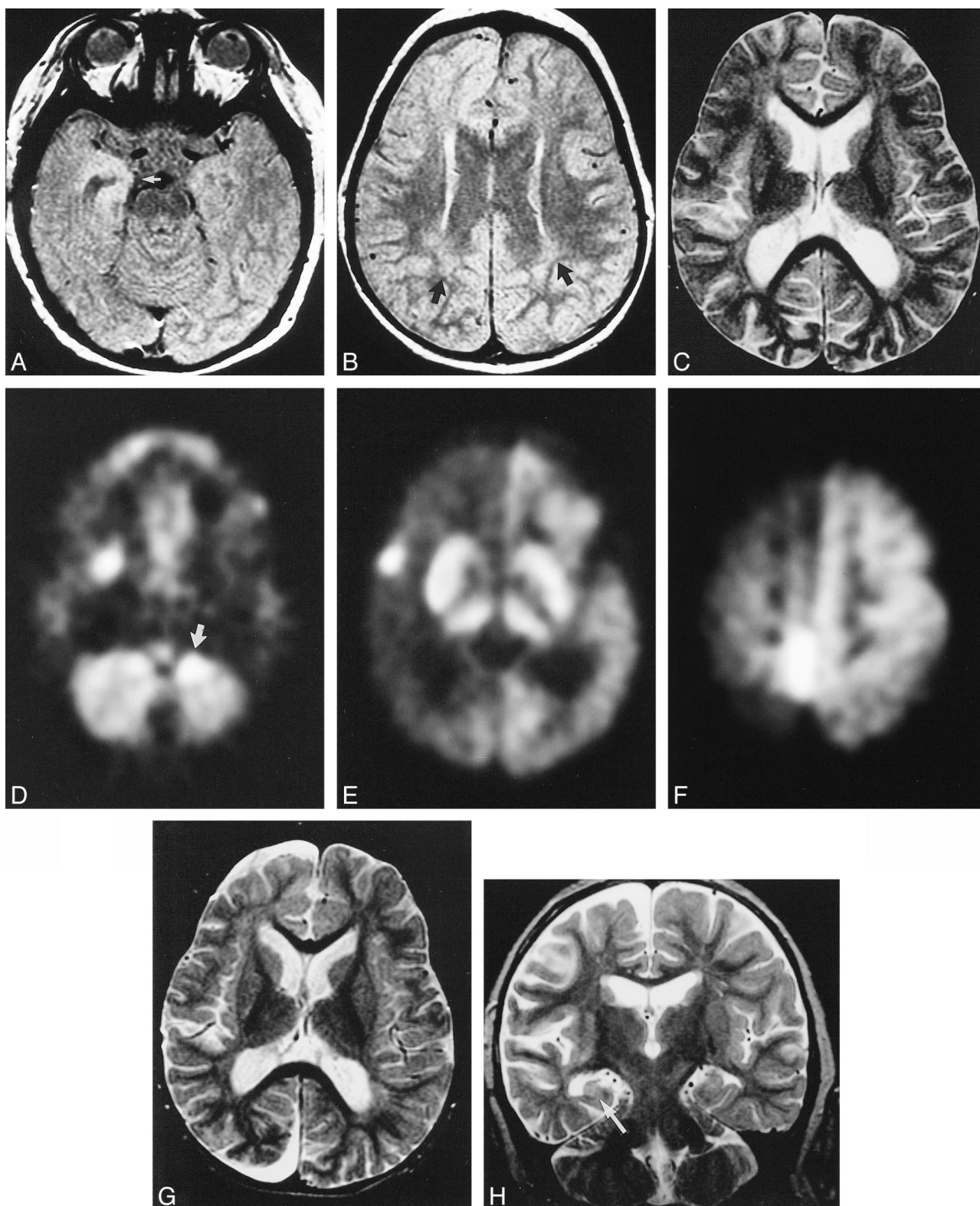


FIG 3. Patient 3, a 27-month-old boy who presented with a 1-year history of intractable seizures followed by a progressive left hemiparesis.

A and B, Axial proton density-weighted images (2800/30/0.75 [TR/TE/excitation]) depict abnormally increased signal in the right medial temporal lobe gray matter (A, *white arrow*), right frontal gray and white matter (B), as well as the posterior white matter bilaterally (B, *black arrows*).

C, Axial T2-weighted image (2800/80/0.75 [TR/TE/excitation]) from the same examination depicts very mild bilateral atrophy, slightly more evident within the right cerebral hemisphere than the left.

D–F, Axial FDG PET images from an examination 5 days later depict global right hemispheric hypometabolism (E, F) with discrete foci of hypermetabolism (indicative of seizure activity at FDG administration) within the medial (D) and lateral (E) right temporal lobe,

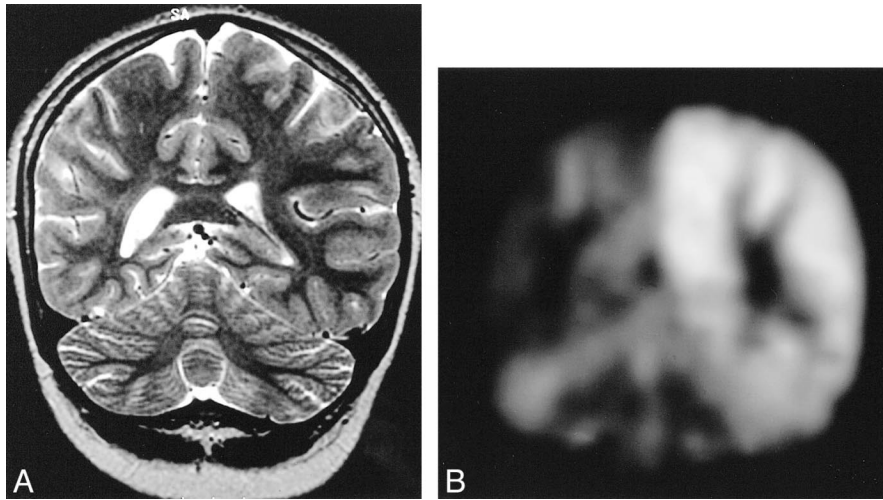


FIG 4. Patient 6, a 9-year-old girl who presented with intractable seizures at age 3.

A, Coronal fast spin-echo T2-weighted image (4000/112/3 [TR/TE/excitations]) through the parietal lobes depicts mild diffuse atrophy of the right cerebral hemisphere, with subtle sulcal prominence and asymmetrical dilation of the body of the right lateral ventricle.

B, Coronal FDG PET image (from a study 5 days earlier) through the same region depicts marked relative hypometabolism within the right cerebral hemisphere (*arrow*). Correlation of the MR imaging data with the FDG PET data and clinical history led to a diagnosis of Rasmussen encephalitis. Analysis of an initial brain biopsy specimen obtained from this patient yielded findings consistent with Rasmussen encephalitis; however, histopathologic analysis from the right hemispherectomy (5 years later) showed only scant perivascular lymphocytic infiltration. This scenario is most consistent with "burned-out" encephalitis. After hemispherectomy, patient 6 became free of seizures and currently requires no antiepileptic medications.

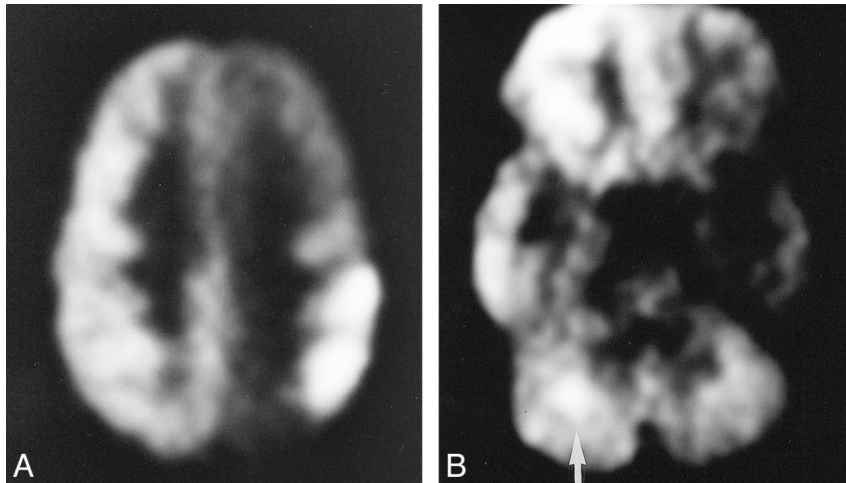


FIG 5. Patient 8, a 7-year-old patient who, at the age of 5, had abrupt onset of intractable seizures (25 to 30 per day).

A and B, Axial FDG PET images depict global left cerebral hypometabolism with superimposed foci of hypermetabolism within the left parietal lobe (A) and right cerebellar hemisphere (B, *arrow*). The patient was actively seizing during injection of the radiopharmaceutical. The pattern of glucose hypermetabolism in this case indicates the propagation of seizure activity from the left parietal cortex to the right cerebellar hemisphere via corticopontocerebellar pathways. This patient underwent brain biopsy followed by left hemispherectomy. The histopathologic specimens from both procedures were interpreted as consistent with Rasmussen encephalitis. Hemispherectomy resulted in resolution of this patient's seizure disorder (at 2-year follow-up).

FIG 3. Continued. medial right parietal lobe (F), anterior left cerebellar hemisphere (D, *arrow*), and right basal ganglia (E). Correlation of the relatively nonspecific MR imaging features with the FDG PET data and clinical history provided a foundation for the diagnosis of Rasmussen encephalitis. In addition, the FDG PET data allowed the unequivocal identification of the affected hemisphere.

G, Axial T2-weighted images from MR imaging study (2800/80/1 [TR/TE/excitation]) 6 months later shows marked progression of the atrophy involving the right cerebral hemisphere, providing further evidence to support the diagnosis of Rasmussen encephalitis and confirm the identification of the affected hemisphere.

H, Fast spin-echo T2-weighted coronal image (4816/110/4 [TR/TE/excitations]) again depicts this asymmetrical (right greater than left) atrophy. In addition, the right hippocampus is atrophied and has abnormally increased T2 signal intensity (*arrow*). Because of the compelling clinical presentation and neuroimaging findings, this patient underwent right hemispherectomy despite two nondiagnostic brain biopsies. Histopathologic findings from the right hemispherectomy specimen were consistent with Rasmussen encephalitis. The disparity between the biopsy and hemispherectomy pathology results may be attributed to "sampling error". This patient is now free of seizures and requires no antiepileptic medications (39 months after hemispherectomy).

may not be involved by the inflammatory process, ie, sampling error. We believe that sampling error occurred in two of our patients, in that the initial biopsy showed either no inflammation or mild, nonspecific inflammatory changes, but subsequent pathologic specimens obtained from hemispherectomy showed findings diagnostic of Rasmussen encephalitis. Second, biopsies performed in the later stages of the disease often show nonspecific findings consisting of only atrophy and residual gliosis with minimal inflammatory cellular infiltrate—referred to as “burned-out encephalitis” by Aguilar and Rasmussen (3). These findings, although consistent with the sequela of an inflammatory process, are nonspecific and can occur after other insults to the brain, such as ischemia or trauma. We believe that this phenomenon of “burned-out encephalitis” was observed in four of the patients in the present series. In two patients, the initial brain biopsies showed unequivocal evidence of active encephalitis, but subsequent hemispherectomy specimens showed only the nonspecific findings that characterize “burned-out” encephalitis. The other two patients presumably had progressed to the “burned-out” encephalitis stage before the initial biopsy. For these reasons, neuroimaging data are often of critical importance in establishing a diagnosis of Rasmussen encephalitis and guiding definitive surgical therapy, particularly in cases of nonspecific clinical findings or discordant or nonspecific histopathologic data.

All patients in the present study had diffuse, unilateral cerebral hypometabolism on FDG PET images, the distribution of which corresponded to equivalent regions of cerebral atrophy on MR images. Unilateral cerebral hypometabolism, in the context of asymmetrical cerebral atrophy on MR images, strongly supports a diagnosis of Rasmussen encephalitis and helps exclude other differential possibilities—hippocampal sclerosis, vascular malformation, neoplasm, cortical dysplasia, or heterotopia—when evaluating a previously developmentally normal child with a new seizure disorder.

We noted two distinct patterns of atrophy in this series of patients. First, we observed a relatively uniform, diffuse pattern of atrophy predominantly involving the cerebral hemisphere that had diffuse hypometabolism on FDG PET images. Second, we found a pattern of focal atrophy superimposed upon a background of diffuse atrophy distributed within the predominantly affected hemisphere. In two of the three cases of focal atrophy, long-TR sequences showed abnormally increased signal intensity within the involved cortex and subcortical white matter. Although we do not have direct histologic correlation, these foci may represent areas of the “destructive encephalitis” described by Aguilar and Rasmussen (3), which are characterized histopathologically by laminar necrosis progressing to spongiform degeneration.

The distribution of cerebral atrophy on MR images closely correlated with the distribution of hy-

pometabolism on FDG PET images in nearly all cases. English et al (8) reported that technetium-99m hexamethylpropyleneamine oxime single-photon emission CT (SPECT) images consistently showed regions of perfusion abnormality that were far more extensive than the corresponding atrophy on neuroimaging studies. This discrepancy between SPECT and CT likely can be attributed to the insensitivity of CT in detecting subtle areas of asymmetrical cerebral atrophy. However, although the distribution of atrophy on MR images often closely matched the distribution of hypometabolism on FDG PET images, subtle diffuse atrophic changes on MR images often were accompanied by marked decreases in cerebral glucose metabolism (Figs 3 and 4). In cases in which the MR imaging findings are subtle, correlation with FDG PET imaging can increase diagnostic confidence and aid in the unequivocal identification of the abnormal cerebral hemisphere.

During ictal studies, patients had multiple foci of hypermetabolism, indicative of seizure activity distributed within the predominantly affected hemisphere. In the current series of patients, the contralateral cerebral hemisphere never showed increased metabolism, which would have suggested propagation of seizure activity across the midline. In the current series of patients, regions of abnormal glucose metabolism (both hypo- and hypermetabolism) were always distributed within the affected cerebral hemisphere, allowing the unequivocal identification of the abnormal side in all patients.

The characteristic pattern of asymmetrical cerebral atrophy and ipsilateral hypometabolism may be accompanied by contralateral cerebellar atrophy and hypometabolism, ie, crossed cerebellar diaschisis, as recently described by Geller et al (9). In the current series, several ictal studies showed hypermetabolic foci within the contralateral cerebellar hemisphere, presumably representing propagation of seizure activity along the corticopontocerebellar pathway (Figs 3 and 5).

Although the histopathologic findings of Rasmussen encephalitis become increasingly nonspecific during the later stages of the disease (3), the radiologic findings in our patients either remained stable or showed gradual progression (Fig 3). Thus, radiologic data may confirm a clinical diagnosis of Rasmussen encephalitis despite nondiagnostic histopathologic findings. Radiologic data are particularly important in patients with discordant results from multiple biopsies, as seen in four of our 11 patients.

Four decades of clinical experience, particularly the reported long-term response to hemispherectomy, have supported the initial observation that Rasmussen encephalitis is, almost exclusively, a focal or unilateral disease process. To our knowledge, only one case of biopsy-proven, bilateral involvement has been reported (3, 4). Therefore, the accurate identification of the abnormal cerebral hemisphere is required for planning the surgical biopsy

and therapy. As previously reported (9, 10), and as indicated by the current data, abnormalities on MR imaging often are bilateral. In our study, nine of 10 patients showed bilateral atrophy, and three patients showed abnormally increased T2 signal bilaterally. In all cases, however, both the atrophy and T2 signal abnormalities were asymmetrical, with predominant involvement of the cerebral hemisphere to which the clinical presentation (seizure activity and hemiparesis or hemiplegia) and abnormal FDG metabolism were localized. The asymmetry in MR imaging abnormalities was sufficient in nearly all of our patients to allow identification of the affected hemisphere on initial examination (Figs 1 and 2). In some cases (Figs 3 and 4), however, the initial MR imaging showed either minimal or no atrophy of the affected hemisphere, or bilateral abnormalities that were only subtly asymmetrical. In these cases, FDG PET data helped to establish the diagnosis and definitively identify the affected side. In contrast to MR imaging, FDG PET imaging showed abnormalities in glucose metabolism that were distributed exclusively within the affected cerebral hemisphere and contralateral cerebellar hemisphere (Figs 1–5). In addition, areas of mild atrophy on MR images often corresponded to markedly abnormal metabolism on FDG PET images (Figs 3 and 4). Thus, although MR imaging alone generally was adequate to identify the affected cerebral hemisphere, FDG PET provided unequivocal, confirmatory data in each case.

The bilateral abnormalities observed on MR images of patients with Rasmussen encephalitis most likely can be attributed in part to the sequelae of the severe, intractable focal seizures (ie, prolonged anoxia and repeated trauma during seizures) and possibly the sequelae of long-term, high-dose antiepileptic medications (10, 11).

The present study has several important limitations. First, this is a retrospective case series and, as such, suffers from an inherent selection bias. Second, only 11 patients were included; the findings in this small series may not reflect the characteristics of all patients with Rasmussen encephalitis. Third, two patients included in the present study lacked pathologic verification of Rasmussen encephalitis. Fourth, the utility of FDG PET imaging to identify bilateral abnormalities is inherently limited. Each patient serves as his own control with the inherent assumption that the unaffected, contralateral cerebral hemisphere is normal. In addition, comparison of each cerebral hemisphere to metabolism within the ipsilateral cerebellum (a frequently applied internal standard) is invalid in the current study, because the cerebellum frequently shows metabolic abnormalities in Rasmussen encephalitis. Finally, no normative data for FDG metabolism are available; as a result, quantitative measures of FDG metabolism vary greatly (owing to fluctuations in arterial-input functions and glucose levels) and are difficult to inter-

pret. Correspondingly, the areas referred to as hypo- or hypermetabolic can be thought of more correctly as “relatively” hypo- or hypermetabolic compared with the corresponding areas of the contralateral hemisphere, which are assumed to have normal glucose metabolism.

Conclusion

The characteristic findings of Rasmussen encephalitis are diffuse, unilateral cerebral hypometabolism on FDG PET images with corresponding regions of cerebral atrophy on MR images. These findings remain stable or gradually progress over time. Supportive imaging findings include: 1) multiple foci of hypermetabolism representative of seizure activity, distributed within the predominantly affected hemisphere and occasionally within the contralateral cerebellar hemisphere during ictal studies, and 2) abnormally increased signal on long-TR sequences, distributed within the white or gray matter of the predominantly involved hemisphere.

In the current series, MR imaging data alone were sufficient in most cases to suggest a diagnosis of Rasmussen encephalitis and to identify the affected cerebral hemisphere. However, FDG PET imaging frequently increased the diagnostic confidence in cases in which the MR imaging findings were subtle, and allowed the unequivocal identification of the abnormal cerebral hemisphere in these cases in which MR imaging abnormalities were bilateral.

References

- Rasmussen T, Olzewski J, Lloyd-Smith D. **Focal seizures due to chronic localized encephalitis.** *Neurology* 1958;8:435–445
- Rasmussen T. **Further observations on the syndrome of chronic encephalitis and epilepsy.** *Appl Neurophysiol* 1978;41:1–12
- Aguilar MJ, Rasmussen T. **Role of encephalitis in pathogenesis of epilepsy.** *Arch Neurol* 1960;2:663–676
- Rasmussen T, McCann W. **Clinical studies of patients with focal epilepsy due to “chronic encephalitis”.** *Trans Am Neurol Assoc* 1968;93:89–94
- Piatt JH, Hwang PA, Armstrong DC, Becker LE, Hoffman HJ. **Chronic focal encephalitis (Rasmussen Syndrome): six cases.** *Epilepsia* 1988;29:268–279
- Rogers SW, Andrews PI, Gahring LC, et al. **Autoantibodies to glutamate receptor GluR3 in Rasmussen’s encephalitis.** *Science* 1994;265:648–651
- Tinuper P, Andermann F, Villemure JG, Rasmussen TB, Quesney LF. **Functional hemispherectomy for treatment of epilepsy associated with hemiplegia: rationale, indications, results and comparison with callosotomy.** *Ann Neurol* 1988;24:27–34
- English R, Soper N, Shepstone BJ, Hockaday JM, Stores G. **Five patients with Rasmussen’s syndrome investigated by single-photon-emission computed tomography.** *Nucl Med Commun* 1989;10:5–14
- Geller E, Faerber EN, Legido A, et al. **Rasmussen encephalitis: Complementary role of multitechnique neuroimaging.** *AJNR Am J Neuroradiol* 1989;19:445–449
- Yacubian EM, Marie SKN, Valerio RME, Jorge CL, Yamaga L, Buchpiguel CA. **Neuroimaging findings in Rasmussen’s syndrome.** *J Neuroimaging* 1997;7:16–22
- Tampieri D, Melanson D, Ethier R. **Imaging of chronic encephalitis.** In: Andermann F, ed. *Chronic Encephalitis and Epilepsy. Rasmussen’s Syndrome.* Boston: Butterworth-Heinemann; 1991: 47–60